15 Absorbable Bone Substitute Materials Based on Calcium Sulfate as Triggers for Osteoinduction and Osteoconduction

Dominik Pförringer and Andreas Obermeier

15.1 Introduction

In times of rising numbers of infections and growing populations bone defects caused by trauma, infection, or tumor pose a challenge for reconstructive surgery. Bone grafting is used as an established method, both autologous and hetero- and xenologous. In addition bone grafts can be antibiotically loaded [1] to prevent or treat infections. The final fate of a bone graft is influenced by local phenomena such as osteocon- and -induction as well as osteogenesis [2]. Autologous grafts are regarded as a near-ideal solution for defect reconstruction. However, their use is not without restrictions, harvesting sometimes complicated and availability limited. An alternative approach for defect reconstruction can be the use of allografts. Research activities have been focused on attempts to create ideal artificial bone grafts. Calcium sulfate (CS) poses a readily available and inexpensive solution with high biocompatibility [3]. In addition CS has the potential for incorporation of therapeutic substances and thus can function as a carrier for drugs, extending its usability in the field of bone reconstruction [4, 5]. Furthermore it can serve as an osteoconductive structure for ingrowing bone, through a process in which newly formed host bone replaces the CS material simultaneously without inducing a significant inflammatory reaction [6]. CS generally has no intrinsic osteoinductive or osteogenic capacity, and its resorption generally happens more rapidly than bone formation [7]. One way to antagonize this is the addition of osteoinductive and/or osteogenic components such as hydroxyapatite (HA) which has proven to deliver favorable results [8, 9]. However, the main limitation for the use of HA ceramics is the inherent brittleness and difficulty in processing [10]. Another promising additive is calcium carbonate. It has been shown that resorption of the CS can leave porosities enhancing the ingrowth of bone. In this study, we analyzed the biological remodeling in response to implantation of new formulations of CS augmented with antibiotics and calcium carbonate/tripalmitin in rabbit tibiae. Bone ingrowth and biomaterial performance were evaluated using optical microscopy, fluorescence microscopy, conventional radiography, and micro-computed tomography (micro-CT). Specifically, the effect of calcium carbonate/tripalmitin formulations of CS on resorption period was examined. Hence, the provision of temporary structural support during the remodeling process, and thus synchronization of the ingrowing bone with biomaterial resorption, as well as preservation of the bone graft's initial volume

D. Pförringer (✉) · A. Obermeier
Klinik und Poliklinik für Unfallchirurgie, Klinikum rechts der Isar, Technische Universität München, Munich, Germany
e-mail: Dominik.Pfoerringer@mri.tum.de; aobermeier@tum.de

D. Duscher, M. A. Shiffman (eds.), *Regenerative Medicine and Plastic Surgery*,
https://doi.org/10.1007/978-3-030-19962-3_15

were investigated. New formulations for delayed resorption and osteoconduction of artificial bone substitute materials may facilitate the bone regeneration process in an antimicrobial environment. Herewith, trauma and orthopedic surgeons may find a future bone substitute material for complex bone regeneration as infect prophylaxis, especially in case of methicillin-resistant staphylococcus aureus (MRSA) infections.

15.2 Materials and Methods

15.2.1 Implants

The resorbable bone substitute materials based on CS formulations used in the experiment consisted of CS dihydrate, gentamicin, and tripalmitin (group 1: Herafill®-G), CS dihydrate, vancomycin, and tripalmitin (group 2: CaSO4-V), as well as commercially available tobramycin-loaded CS hemihydrate (group 3: Osteoset®). The specific beads varied in size and consequently in implanted quantity to match overall implanted mass of approximately 500 mg. For this purpose, two units of group 1 implants (500 mg), 14 units of group 2 implants (490 mg), and five units of group 3 (537.5 mg) were used to implant inside an artificial rabbit tibial bone defect for investigation.

Group 1 implants at 6.0 mm diameter and 250 mg weight per unit consist of calcium sulfate dihydrate (71.6%), calcium carbonate (17.9%), tripalmitin (8.8%), and gentamicin sulfate (1.7%). Group 2 implants at 3.0 mm diameter and 35 mg per unit consist of calcium sulfate dihydrate (72.0%), calcium carbonate (18.0%), tripalmitin (8.9%), and vancomycin hydrochloride (1.1%). Group 3 implants at 4.8 mm diameter and 107.5 mg weight per unit consist of a hemihydrate modification of calcium sulfate (96.0%) and tobramycin sulfate (4.0%). Composition of bead implants is given in contents per weight.

15.2.2 Animal Study: Protocol

The study was approved by the Animal Experimentation Ethics Committee of Bavaria (Reg. No. 209.1/211-2531.2-22/05) and conducted with reference to the OECD Principles of Good Laboratory Practice. Fifty-four female New Zealand white rabbits (Charles River Laboratories, Sulzfeld, Germany) with a mean body weight (BW) of 4.5 kg (range: 4.3–4.7 kg) underwent surgery. For acclimatization purposes, the animals were delivered to the facility at least 2 weeks prior to surgical intervention. Animals were housed in cages (2–3 animals) at normal room temperature and daylight illumination with ad libitum access to food and water. The animals were divided into three groups according to the test implant groups (Fig. 15.1).

15.2.3 Animal Study: Surgical Procedure

The surgical procedure was performed under general anesthesia utilizing weight-adapted intramuscular injection of medetomidine 0.25 mg/kg BW (Domitor®, Pfizer Inc., Germany) and ketamine 17 mg/kg BW (S-Ketanest®, Parke-Davis GmbH). Analgesia during surgery was obtained through intravenous application of metamizole 30 mg/kg BW (Novaminsulfon®, Ratiopharm GmbH, Germany) at the beginning of surgery. The left hind leg prior to surgery was shaved, and the skin cleaned antiseptically (Cutasept®, Bode Chemie, Germany). The skin incision was placed laterally of the tibial tuberosity; consequently bone manipulation was performed at the medial side. This local skin displacement serves the purpose of infection prevention through the skin wound. A water-cooled surgical diamond fraise was employed to drill an 8 mm spherical bone cylinder to open the medullary cavity. Using a sterile forceps beads were inserted into the proximal medullary cavity. Specific quantities of implants were implanted according to varying size of beads to match overall implanted mass of 500 mg (±8%) (group 1: 2 units, group 2: 14 units, and group 3: 5 units). After implantation, the cavity was closed using the initially removed bone cylinder while surgical site was irrigated using sterile saline. Subcutaneous tissues were readapted (3-0 Vicryl®, Ethicon GmbH, Germany), and skin closed (3-0

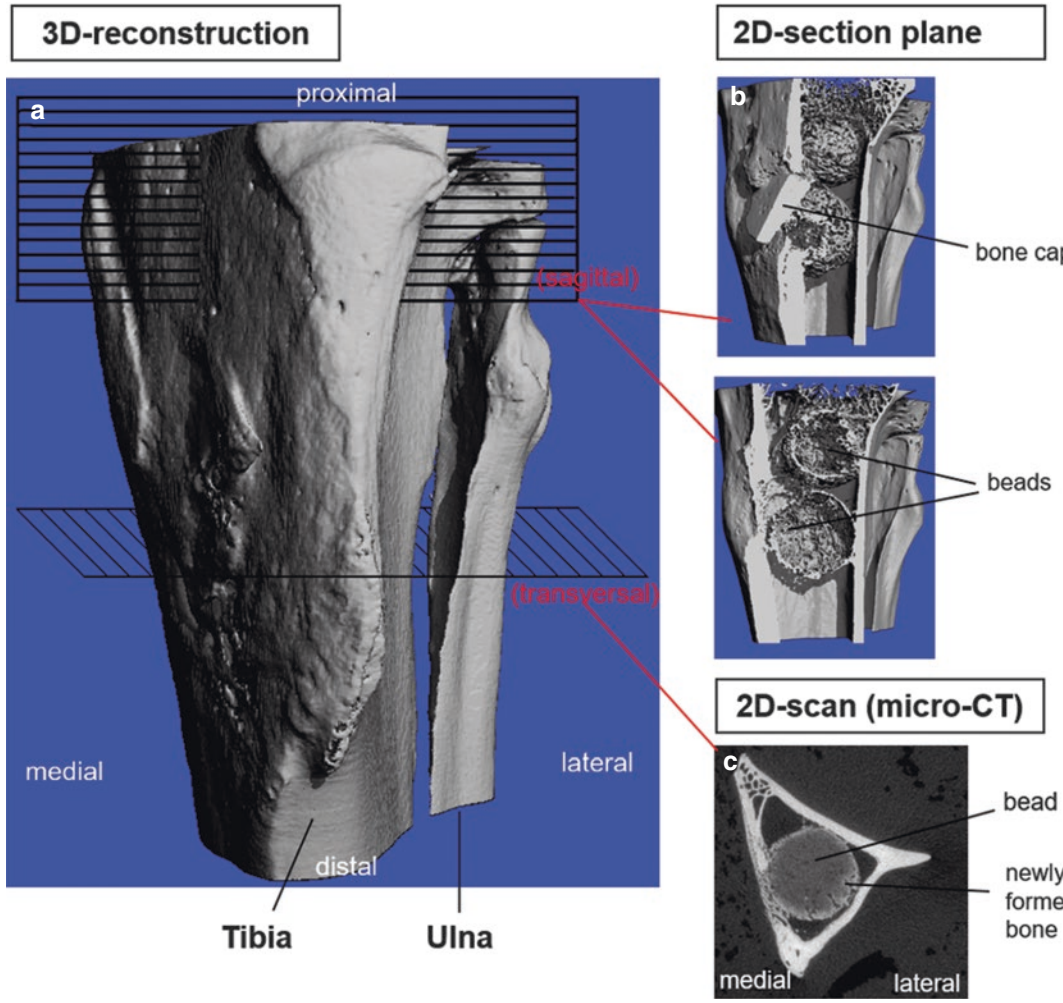

Fig. 15.1 Explanation of micro-CT planes used for tibia of a sacrificed animal (group 1 after 6 weeks). Exemplary declaration of micro-CT planes used in sacrificed rabbits from group 1 after 6 weeks: (**a**) 3-D reconstruction was carried out for gross overview; 2-D section plane in the sagittal direction (**b**) and the transversal plane from micro-CT scan (**c**) were analyzed for bone ingrowth and implant degradation. Reproduced with permission

Prolene®, Ethicon GmbH, Germany). Thereafter, a spray bandage (Opsite®, Smith & Nephew PLC, England) was applied. Anesthesia was antagonized using atipamezole 0.25 mg/kg (Antisedan®, Pfizer Inc., Germany).

Buprenorphine (0.03 mg/kg BW s.c., Temgesic®, Essex Pharma GmbH, Germany) was administered for analgesia towards the end of the surgical procedure immediately before wound closure was completed and postoperatively every 8 h for 4 days. In addition, carprofen 4 mg/kg s.c. (Rimadyl®, Pfizer Inc., Germany) was given for 7 days every 12 h. Animals underwent daily control examinations considering general condition, body temperature, and surgical site of the operated leg. Blood was obtained from the ear vein towards the end of the surgical procedure and weekly until sacrifice of the animal to determine blood count, and calcium/alkaline phosphatase levels.

Animals were euthanized after 4, 6, 8, and 12 weeks according to different testing groups employing an overdose of pentobarbital-sodium (Narcoren®, Merial GmbH, Germany 50 mg/kg). The tibiae were dissected. Then, all soft tissue was stripped from the bone, which was consecutively stored in 100% methanol.

15.2.4 Radiographic Evaluation

Immediately after surgery and at the end of each observation period, the tibiae underwent X-ray via contact radiography in a lateral view using an X-ray generator at 44 kV and 4 mAs (Super 80CP, Philips GmbH, Germany). Evaluation of the imaging changes was performed semiquantitatively.

15.2.5 Micro-CT

In addition, micro-computed tomography (micro-CT 80, Fa. Scanco, Brüttisellen, Switzerland) of the explanted tibiae was carried out. Images were obtained as transverse planes of the tibia and were further processed as 3-dimensional reconstructions to get an overview. All micro-CTs were performed after sacrifice of the animals on dissected tibiae.

15.2.6 Histology

Histomorphological analysis (Fig. 15.2) was performed to evaluate bone growth and bone vitality around the implants using two kinds of staining. In vivo fluorochrome substances were injected postoperatively at fixed time intervals to achieve a fluorescent labeling of newly formatted bone. Additionally, a classical histomorphological staining of specimen surfaces was performed after polymerization and down polishing of tibiae ex vivo.

Histological specimens were prepared by embedding with methyl-methacrylate resin (Technovit® 4004,HeraeusKulzer GmbH, Germany) and dissecting mid-tibiae sagittally utilizing a diamond saw (Exakt 300CL, Exakt GmbH, Germany), followed by grinding down with a polishing machine (Planopol-V and Pedemax-2, Struers GmbH, Germany) to a

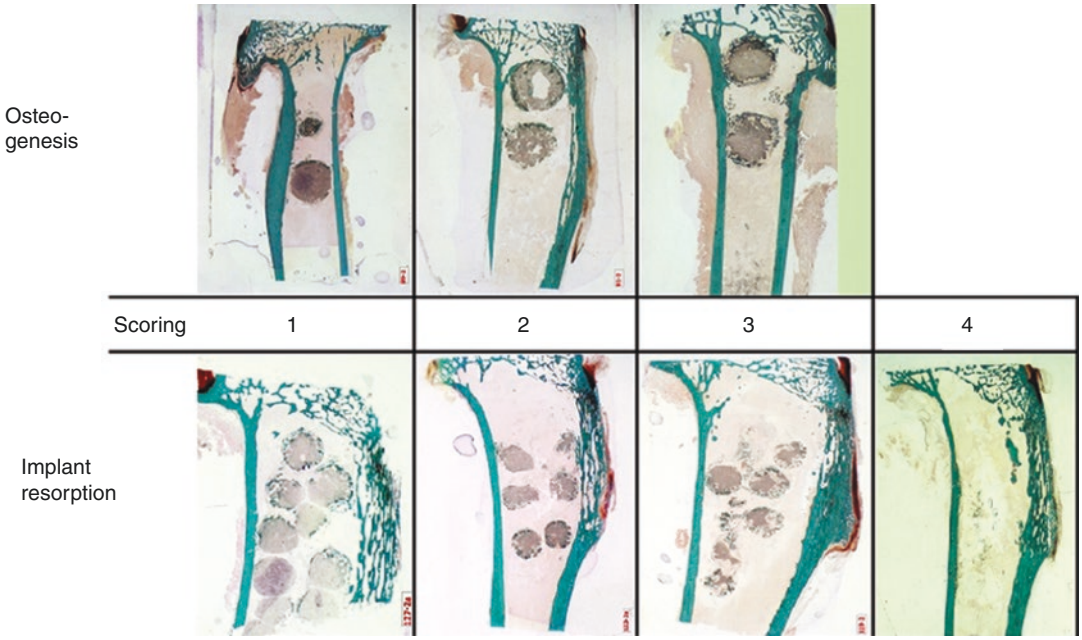

Fig. 15.2 Histological scoring system (modified Giemsa stain) for osteogenesis (group 1) and implant resorption (group 2). Histological scoring system (modified Giemsa stain) for osteogenesis (*1*: no osteogenesis, *2*: <50% of implant circumference with signs of osteogenesis, *3*: >50% of implant circumference with signs of osteogenesis) and implant resorption (*1*: <10% of implant degraded, *2*: 10–50% of implant degraded, *3*: >50% of implant degraded, *4*: <10% of implant remnants detectable). Reproduced with permission

thickness of 40–120 µm with diamond discs to get histological slides.

Approximately 100 µm thick tibia sections of every group at 4, 6, 8, and 12 weeks were then histomorphologically stained with a modified Grünwald-Giemsa staining called "K2." This staining is suitable to evaluate the newly formed bone, with newly formed osteoid tissue stained yellowish-brown, old bone stained light-green/blue, connective tissue stained orange-red, and calcifications stained bright-greenish-blue. The surface-stained specimens were then investigated via photo macroscopy (Wild M400, Wild Heerbrugg AG, Switzerland) at ×2 magnification to get an overview and using light microscopy (DMRB, Leica Microsystems GmbH, Germany) for more detail at ×25 and up to ×250 magnifications.

All implants and surrounding tissue were evaluated for osteogenesis (criteria: amount of trabecular bone formation, number of osteoblasts, amount of osteoid, general impression) and amount of implant resorption (criteria: lysis of implant surface, presence and number of surrounding giant cells, general inspection of morphology). Osteogenesis was graded on a scale from 1 to 3 (little to maximum), and resorption of implants from 1 to 4 (none to complete).

To measure bone apposition rates after surgery (i.e., the rate of bone ingrowth or bone deposition) within and around the implants, five separate fluorochrome labels were administered subcutaneously. For this purpose different fluorochrome solutions were injected at the following days postoperatively: 21 and 22 days (tetracycline, 30 mg/kg BW), 35 and 36 days (alizarin complexone, 30 mg/kg BW), 49 and 50 days (calcein green, 30 mg/kg BW), 63 and 64 days (xylenol orange, 90 mg/kg BW), and 77 and 78 days (calcein blue, 30 mg/kg BW). Fluorochrome labels are bound to sites of active bone deposition shortly after administration [11]. Therefore, the time of bone formation can be related to the individual fluorescence color of each fluorochrome label administered chronologically.

Later on, specimens were investigated with their fluorochrome labeling, because of new bone formation using a light microscope (DMRB, Leica Microsystems GmbH, Germany) with an ultraviolet light source and at ×25 and up to ×250 magnifications. Polychrome sequence marking was performed during the time of postoperative observation, exemplarily for one animal of each group. The fluorescence evaluation was performed at weeks 8 and 12.

Table 15.1 Correlation of fluorescence color and bone formation time

Substance	Time of bone formation (postoperative week)	Fluorescence color (UV excitation)
Tetracycline	3	Yellow/green
Alizarin complexone	5	Red
Calcein green	7	Green
Xylenol orange	11	Orange

Correlation of fluorescence color of newly formed bone dependent on substance solution and time of administration used. Resulting in visually distinguishable stains of newly formed bone at different time periods by defined colors

Fluorescence colors of bone tissue specimens indicate the time of bone formation, correlating with the time of fluorescence stain application in vivo. Thus, time of bone formation can be assigned to individual label colors.

15.2.7 Statistical Analysis (Table 15.1)

Experimental investigations via X-ray, micro-CT, and classical histology were conducted on a minimum of four animals. One animal for each group was sacrificed additionally at weeks 8 and 12, to achieve specimen for fluorescence microscopy after polychrome sequence labeling. Scores for X-rays and classical histological (modified Giemsa stain) pictures were generated to collect semiquantitative information on the progress of implant resorption and osteogenesis.

15.3 Outcome and Scientific Literature Context

Rapid and complete reconstruction of bone defects through autologous or allogeneic bone or bone-related tissue can be crucial in trauma

and orthopedic surgery. Calcium sulfate (CS), also known as plaster of paris, has been used for multiple implications for more than a century [12] and its use in the surgical setting has been proposed [2]. Key features of this bone graft substitute include its biocompatibility as well as its features as a binding and stabilizing agent. Additionally it can serve osteoconductive purposes potentially leading to bone ingrowth [13, 14]. On the other hand, rapid resorption rate limits its use as a structural allograft. In this context, some authors found unsatisfactory results for CS if used as a bone graft [15]. We had anticipated that a combination of CS with calcium carbonate/tripalmitin can purposely delay the degradation process, providing temporary structural support during remodeling, synchronizing the ingrowing bone with biomaterial resorption, as well as preserving the bone grafts' initial volume. This study aimed to visualize the mechanisms of bone formation in the presence of novel antibiotic-impregnated CS implants in a rabbit model. With the use of radiographic and histologic methods, none of the three tested bead formulations (Herafill®-G (1), CaSO4-V (2), and Osteoset® (3)) displayed any adverse reactions, while all of them were undergoing at least partial decomposition within the tibial bone.

In the underlying research the surgical procedure was well tolerated by all rabbits as well as the follow-up period. The animals were immediately after surgery fully weight bearing. No local or generalized signs of infection were observed.

These three bone substitutes composed of CS; differing side groups consisting of dihydrate (1, 2) and hemihydrate (3) in combination with differing antibiotics (gentamicin (1), vancomycin (2), and tobramycin (3)) were used as study implants. Beads of group 3 consisted of a hemihydrate formulation of CS and are commercially available (Osteoset®). In contrast, beads of groups 1 and 2 are novel preparations consisting of CS dihydrates with calcium carbonate and tripalmitin. Also, group 1 (Herafill®-G) is a commercial product, whereas group 2was at the time of testing still in the development stage to treat MRSA infections in the future. The rationale for the use of calcium carbonate as an additive is its ability to delay degradation of CS and buffer the pH value in the implant region, thus counteracting healing problems of the tissue [16, 17]. Tripalmitin as a fatty acid influences the release kinetics of the antibiotics gentamicin and vancomycin to allow the beads to act potentially antimicrobially over a longer period of time [18, 19].

The tibiae were analyzed by different methods, in which drug release kinetics had already been described [12]. Conventional radiographs allowed a statement on the rate of resorption of implants during the study period. Further examination by micro-CT enabled a more precise insight into the processes of bone formation and implant resorption. While the 3-D reconstructions gave an overview of the processes in the interior of the entire bone, the main disadvantage is the influence on the image by adjusting black-and-white values. On the other hand, the transversal 2-D images reflect the unaltered facts and ongoing visible mechanisms at the bone-implant interface. However, the amount of pictures is not suitable for an overview. Therefore, the combination of both views is essential for analysis of the mechanisms acting around the implants.

15.4 Resulting Radiographic Imaging

Conventional X-ray imaging showed differences of biodegradation between the implants over time. Initially, 4 weeks after implantation, all beads were radiographically detectable at the level of the initial insertion sites. Evaluation of changes in radio-opaqueness revealed no relevant changes from the 4th to the 12th weeks, with well-distinguishable beads at 12 weeks in group 1. Radiolucency of the beads increased over the study period in groups 2 and 3. In group 2 radiolucency increased uniformly starting from the 4th week with completely disbanded implants at 12 weeks. In group 3 the implants were only faintly detectable after the 4th week and had already disappeared radiologically after 6 weeks.

15.4.1 Micro-CT

In group 1 all investigated implants showed radiopaque cores and localized mineralized surface changes after 4 weeks. Two of four animals showed beads with well-distinguishable trabecular structures between the implant's surface and the host bone cortex. After 6 weeks the radiopaque core of all implants had disappeared, and the resorption left a homogenously disorganized surface. In addition, cortical bone bridges reached all implants. After 8 and 12 weeks, bone bridging on the implants had progressed, with no change in resorption of the implants.

Almost complete resorption for groups 2 and 3 was detected within 12 and 6 weeks, respectively. The implants were almost completely resorbed in all animals. Varying degrees of mineralization at the periphery of the implant bed were detected. Group 2 indicated a delayed resorption until week 12 and superficial trabecular structures, compared to pure calcium sulfate. Bone bridges from the animals' cortex to the mineralized areas were found in a smaller quantity in group 2, but not for group 3 implants.

Resorption of the beads between the groups of this study differed considerably. The implants of group 3 consisted only of CS and tobramycin and had already shown peripheral and central signs of resorption in the 4th week. In the 6th and especially the 8th weeks after implantation, beads had almost fully degraded. Beads of group 2 were no longer detectable radiologically after the 12th week, while the micro-CT scans and histological slices showed remnants of the beads as well as low amounts of bone formation around the former implant sites. This observation was supported by the data of the polychrome sequence marking. The beads of group 1 (Herafill®-G) were well detectable radiographically after 4 weeks. In the 6th week increasing radiolucency of the beads was detectable, which increased up to week 8. At week 12 no further changes had shown. These observations suggest that both the size and composition of the implants influence the degradation rate. For Osteoset®, CS alone (group 3), a faster degradation was observed than for the compositions containing tripalmitin and calcium carbonate (groups 1 and 2 ($CaSO_4$-V)). Within the latter group, the size of the implants seems to play an important role, since the small beads of group 2 were absorbed more rapidly than the large beads of group 1. These findings are in accordance to reported data from literature, where different degradation times for CS are reported for different sizes of implants: 3–4 weeks [20], 4–10 weeks [21], 6 weeks [22], 5–7 weeks [23], 45–72 days [3, 24], 8 weeks [25], 2–4 months [16], and 6 months [26]. This shows that size correlates directly with resorption time. Additionally, the localization of implantation influences degradation time as presented on beads in the radius [3], tibia [27], femur [27], or maxilla and mandible [28, 29]. Lastly, the used animal model can also influence the degradation as already investigated in the dog [3, 28, 29] or rabbit [20].

15.5 Histological Results

In group 1, trabecular bone formation, invasion of osteoblasts, and erosion were detectable on all implants' surfaces after 4 weeks. These mechanisms protruded up to 12 weeks with still detectable implants and surrounding giant cells at the time of sacrifice. In group 2, changes described above for group 1 were visible after 4 weeks as well. Implant resorption was more pronounced compared to group 1 with almost fully degraded implants after 12 weeks. Giant cells were not detectable from week 8 on. Group 3 showed similar osteogenesis as group 2 with invasion of osteoblasts and production of osteoid starting from week 4. Resorption was very pronounced with almost fully resorbed implants from week 6 on. No more beads were recognizable after 12 weeks.

Analysis of the histological specimen by means of polychrome sequence marking after 8 and 12 weeks revealed the peri-implant bone as newly formed vital bone with enhancement of applied fluorochromes (Fig. 15.3). In the newly formed bone, no evidence of foreign-body response to the biomaterials (e.g., presence of inflammatory cells or fibrous tissue) was observed.

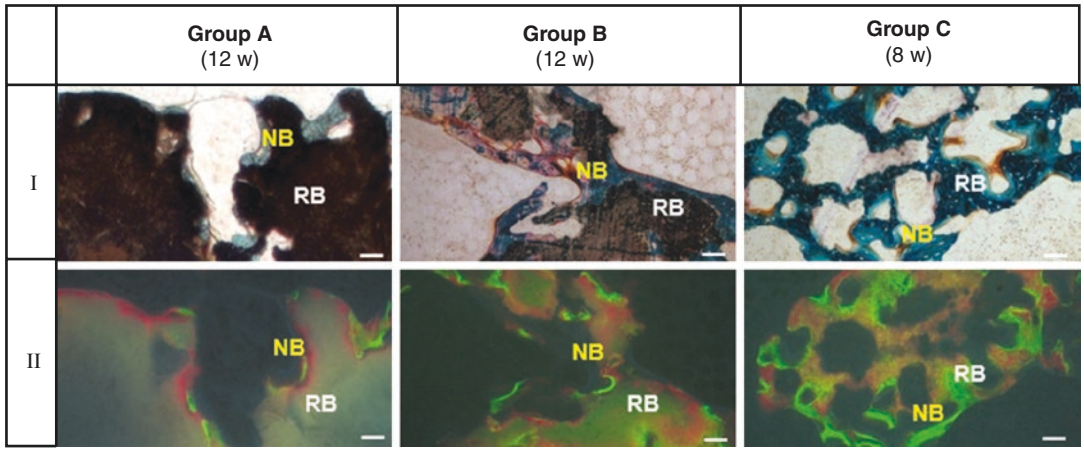

Fig. 15.3 Histological slices and fluorochrome-labeled bone at the implants in tibia of each group. Histological slices (*I*) and fluorochrome-labeled bone (*II*) of tibia of each group 1–3 after 12 weeks (1: Herafill®-G and 2: CaSO4-V), as well as after 8 weeks (3: Osteoset®). Corresponding to histological pictures fluorochromes were deposited around and inside the beads (*NB* new bone, *RB* remnants of beads). (*II*) Fluorescence colors indicate newly formed bone at different postsurgical periods (yellow/green (3w): tetracycline; red (5w): alizarin complexone; green (7w): calcein green; orange (11w): xylenol orange). The white scale bars represent 100 μm length. Reproduced with permission

By means of histological staining in the present study, we were able to find deep lacunae in the peri-implant bone of all three formulations as clear signs of cellular degradation. Additionally, the presence of multinucleated giant cells on or in the implant material confirms the presence of cellular degradation. Regarding the nature of CS degradation contradicting mechanisms have been described. Bell et al. and Tay et al. argue that CS degrades through the process of dissolution [23, 25]. This supports other investigators, who explain accelerated bone formation by provision of calcium ions during the degradation process [20]. Walsh et al. [30] conclude that the pH reduction leads to a demineralization of the adjacent bone, which subsequently leads to a release of BMP, which in turn stimulates bone regeneration. Sidqui et al. [31] also noted in their study that the activity of osteoclasts was excited by an acidic pH. Other authors however argue that CS is degraded by cellular phagocytosis [3]. Orsini et al. [32] report in their study a combination of both dissolution and cell-mediated degradation of CS [32]. However, whether CS additionally is degraded by dissolution cannot be stated with the findings of the present study.

The osteoconductive potential of CS was clearly detected in this study. All three formulations showed invading osteoblasts with active production of osteoid at the implant sites and walled osteocytes with surrounding newly formed bone at the level of the implants' surfaces and in the resorption lacunae. Group 3 showed osteogenesis up to the 8th week, with only remnants of osteoid at the level of the former implant site up to the 12th week (Fig. 15.4). Similar events were found in group 2, with active osteogenesis from the 4th week starting and decreasing over time. Group 1 beads seemed to induce osteogenesis at a steady-state level from the 4th up to the 12th weeks. Here, fine cortical bone trabeculae bridged the implant-bone interface at the day of sacrifice. Possibly, the osteoconductive effect of group 2 may be improved to the level of group 1 by using larger bead dimensions. In summary, osteogenesis was found to decrease over time in groups 2 and 3 almost parallel to degradation of the beads. On the other hand, high levels of osteogenesis in group 1 were detected over 12 weeks. These mechanisms were also supported by polychrome sequence marking after 12 weeks. In all three formulations, clear osteogenic signs detecting bone formation in direct contact to the degrading implants were found.

One limitation of this study is the use of different sizes for implants employed. The weights of the beads in sum were comparable accordingly

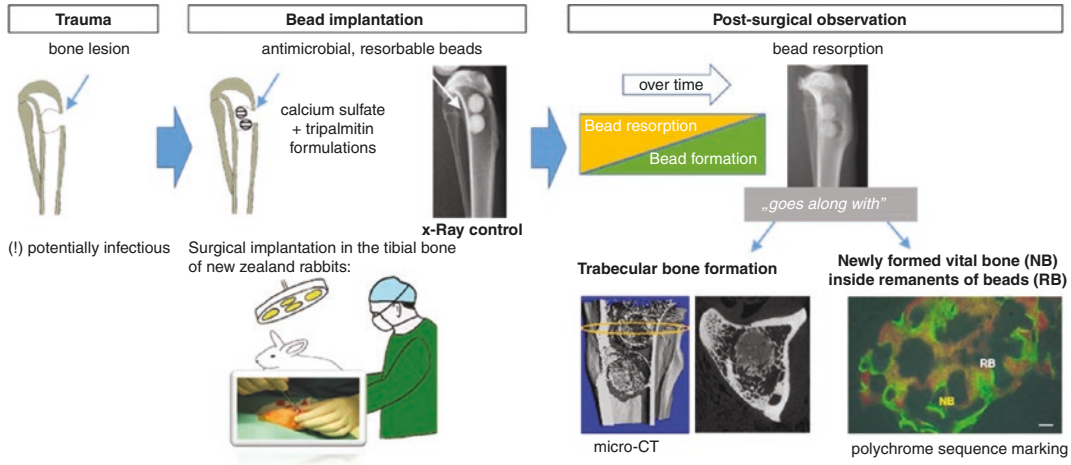

Fig. 15.4 Graphical abstract: experimental method overview. Reproduced with permission

using different numbers of beads per type. To allow for an ideally comparable situation, beads of exact same size and antibiotic content should be used. However, this study delivers valid results for resorption and bone formation over time, as the use of real market-ready material was compared. Molecular biologic methods in future studies might help in further evaluation of the newly formed bone inside and around the implants during resorption.

In summary, this study supported the biocompatibility of novel antibiotic-impregnated CS beads and specified the mechanisms in a rabbit model. The addition of calcium carbonate/tripalmitate delayed the degradation of the implants and resulted in synchronization of the ingrowing bone with biomaterial resorption but did not have negative effects on biocompatibility. Further in vivo studies are needed, in order to estimate time for complete resorption of these new formulations of CS beads and to determine responses of bone cells to this biomaterial.

15.6 Outlook

In a rabbit model novel formulations of absorbable bone substitute materials based on calcium sulfate exhibit delayed time of resorption, while osteoconduction is facilitated. Moreover, a sustaining osteogenic effect is determined over 12 weeks after implantation for Herafill®-G beads. The use of novel calcium sulfate-based bone substitute materials, incorporated with calcium carbonate/tripalmitin and antibiotics, can stimulate the bone regeneration process in an antimicrobial environment. Herewith, trauma and orthopedic surgeons may receive a future bone substitute material for complex bone regeneration as well as infection prophylaxis.

Acknowledgments At first, we would like to thank Mr. Dr. H. Büchner and Mr. Dr. S. Vogt (Heraeus Medical GmbH, Wehrheim, Germany) for their kind supply of bone substitute materials (Herafill®-G, as well as CaSO4-V). Second, many thanks to the central preclinical research division (ZPF) of the Klinikum rechts der Isar at the Technical University of Munich for their excellent support in performing the animal study. Especially, many thanks to Mrs. Dr. M. Rößner and Prof. Dr. H. Gollwitzer for their guidance in surgical procedure. Also, many thanks to Mrs. Dr. S. Kerschbaumer for generating and interpreting histological slices. Moreover, special thanks to Prof. Dr. P. Augat (Department of Biomechanics at the Unfallklinik Murnau) for his kind support in micro-CT investigations. Our special gratitude goes to Dr. Meredith Kiokekli for co-conduction of the experiments as well as to Mr. F. Seidl (M.A. Interpreting and Translating, MBA) for his kind support due to his perfect command of scientific English.

Disclaimer: Parts of this scientific article have by the authors previously been published in Journal of Material Science Materials in Medicine (Springer International Publishing AG). Reproduction was permitted by Springer.

References

1. Lalidou F, Kolios G, Drosos GI. Bone infections and bone graft substitutes for local antibiotic therapy. Surg Technol Int. 2014;24:353–62.
2. Cortez PP, Silva MA, Santos M, Armada-da-Silva P, Afonso A, Lopes MA, Santos JD, Maurício AC. A glass-reinforced hydroxyapatite and surgical-grade calcium sulfate for bone regeneration: in vivo biological behavior in a sheep model. J Biomater Appl. 2012;27(2):201–17.
3. Peltier LF. The use of plaster of paris to fill large defects in bone. Am J Surg. 1959;97(3):311–5.
4. Helgeson MD, Potter BK, Tucker CJ, Frisch HM, Shawen SB. Antibiotic-impregnated calcium sulfate use in combat-related open fractures. Orthopedics. 2009;32(5):323.
5. Beuerlein MJ, McKee MD. Calcium sulfates: what is the evidence? J Orthop Trauma. 2010;24(Suppl 1):S46–51.
6. Thomas MV, Puleo DA. Calcium sulfate: properties and clinical applications. J Biomed Mater Res B Appl Biomater. 2009;88(2):597–610.
7. Slater N, Dasmah A, Sennerby L, Hallman M, Piattelli A, Sammons R. Back-scattered electron imaging and elemental microanalysis of retrieved bone tissue following maxillary sinus floor augmentation with calcium sulphate. Clin Oral Implants Res. 2008;19(8):814–22.
8. Parsons JR, Ricci JL, Alexander H, Bajpai PK. Osteoconductive composite grouts for orthopedic use. Ann N Y Acad Sci. 1988;523:190–207.
9. Stubbs D, Deakin M, Chapman-Sheath P, Bruce W, Debes J, Gillies RM, Walsh WR. Biomaterials. 2004;25(20):5037–44.
10. Fan X, Ren H, Luo X, Wang P, Lv G, Yuan H, Li H, Yan Y. Mechanics, degradability, bioactivity, in vitro, and in vivo biocompatibility evaluation of poly(amino acid)/hydroxyapatite/calcium sulfate composite for potential load-bearing bone repair. J Biomater Appl. 2016;30(8):1261–72.
11. Frost HM. Tetracycline-based histological analysis of bone remodeling. Calcif Tissue Res. 1969;3(3):211–37.
12. Pforringer D, Obermeier A, Kiokekli M, Büchner H, Vogt S, Stemberger A, Burgkart R, Lucke M. Antimicrobial formulations of absorbable bone substitute materials as drug carriers based on calcium sulfate. Antimicrob Agents Chemother. 2016;60(7):3897–905.
13. Borrelli J Jr, Prickett WD, Ricci WM. Treatment of nonunions and osseous defects with bone graft and calcium sulfate. Clin Orthop Relat Res. 2003;411:245–54.
14. Evaniew N, Tan V, Parasu N, Jurriaans E, Finlay K, Deheshi B, Ghert M. Use of a calcium sulfate-calcium phosphate synthetic bone graft composite in the surgical management of primary bone tumors. Orthopedics. 2013;36(2):e216–22.
15. Glazer PA, Spencer UM, Alkalay RN, Schwardt J. In vivo evaluation of calcium sulfate as a bone graft substitute for lumbar spinal fusion. Spine J. 2001;1(6):395–401.
16. Coetzee AS. Regeneration of bone in the presence of calcium sulfate. Arch Otolaryngol. 1980;106(7):405–9.
17. Coraca-Huber D, Hausdorfer J, Fille M, Nogler M, Kuhn KD. Calcium carbonate powder containing gentamicin for mixing with bone grafts. Orthopedics. 2014;37(8):e669–72.
18. Coraca-Huber DC, Putzer D, Fille M, Hausdorfer J, Nogler M, Kuhn KD. Gentamicin palmitate as a new antibiotic formulation for mixing with bone tissue and local release. Cell Tissue Bank. 2014;15(1):139–44.
19. Obermeier A, Matl FD, Schwabe J, Zimmermann A, Kühn KD, Lakemeier S, von Eisenhart-Rothe R, Stemberger A, Burgkart R. Novel fatty acid gentamicin salts as slow-release drug carrier systems for anti-infective protection of vascular biomaterials. J Mater Sci Mater Med. 2012;23(7):1675–83.
20. Lebourg L, Biou C. The imbedding of plaster of paris in surgical cavities of the maxilla. Sem Med Prof Med Soc. 1961;37:1195–7.
21. Geldmacher J. Therapy of enchondroma with a plaster implant—renaissance of a treatment principle. Handchir Mikrochir Plast Chir. 1986;18(6):336–8.
22. Petruskevicius J, Nielsen S, Kaalund S, Knudsen PR, Overgaard S. No effect of Osteoset, a bone graft substitute, on bone healing in humans: a prospective randomized double-blind study. Acta Orthop Scand. 2002;73(5):575–8.
23. Bell WH. Resorption characteristics of bone and bone substitutes. Oral Surg Oral Med Oral Pathol. 1964;17:650–7.
24. Lillo R, Peltier LF. The substitution of plaster of Paris rods for portions of the diaphysis of the radius in dogs. Surg Forum. 1956;6:556–8.
25. Tay BK, Patel VV, Bradford DS. Calcium sulfate- and calcium phosphate-based bone substitutes. Mimicry of the mineral phase of bone. Orthop Clin North Am. 1999;30(4):615–23.
26. Kelly CM, Wilkins RM, Gitelis S, Hartjen C, Watson JT, Kim PT. The use of a surgical grade calcium sulfate as a bone graft substitute: results of a multicenter trial. Clin Orthop Relat Res. 2001;382:42–50.
27. Blaha JD. Calcium sulfate bone-void filler. Orthopedics. 1998;21(9):1017–9.
28. Calhoun NR, Greene GW Jr, Blackledge GT. Plaster: a bone substitute in the mandible of dogs. J Dent Res. 1965;44(5):940–6.
29. McKee JC, Bailey BJ. Calcium sulfate as a mandibular implant. Otolaryngol Head Neck Surg. 1984;92(3):277–86.

30. Walsh WR, Morberg P, Yu Y, Yang JL, Haggard W, Sheath PC, Svehla M, Bruce WJ. Response of a calcium sulfate bone graft substitute in a confined cancellous defect. Clin Orthop Relat Res. 2003;406:228–36.
31. Sidqui M, Collin P, Vitte C, Forest N. Osteoblast adherence and resorption activity of isolated osteoclasts on calcium sulphate hemihydrate. Biomaterials. 1995;16(17):1327–32.
32. Orsini G, Ricci J, Scarano A, Pecora G, Petrone G, Iezzi G, Piattelli A. J Biomed Mater Res B Appl Biomater. 2004;68(2):199–208.